

^{35}Cl nuclear-quadrupole-resonance investigations of the lock-in phase and of the new low-temperature phase in K_2ZnCl_4

F. Milia

Nuclear Research Center Demokritos, Athens, Greece

R. Kind and J. Slak*

*Laboratory of Solid State Physics, Swiss Federal Institute of Technology,
Hönggerberg, CH-8093 Zürich, Switzerland*

(Received 29 September 1982)

The ferroelectric lock-in phase III and the new low-temperature phase IV of K_2ZnCl_4 are analyzed by means of ^{35}Cl NQR measurements combined with group-theoretical considerations. It is shown that the eigenvector of the frozen-in soft mode in phase III, which consists mainly of rotations of the ZnCl_4 tetrahedra around the pseudo-hexagonal a axis, is very big compared to Rb_2ZnCl_4 . The amplitude of the frozen-in rotation wave is measured to be 79° at 200 K. In the new low-temperature phase, a quadruplication of the NQR lines is observed which can be explained by a zone-boundary transition leading to a monoclinic phase. A possible influence of the domain pattern upon the NQR-signal amplitude, originating from phase solitons which survived the lock-in transition, is discussed.

INTRODUCTION

K_2ZnCl_4 is a typical example of a one-dimensionally modulated incommensurate system of the $A_2\text{BX}_4$ family. It is well known^{1,2} that K_2ZnCl_4 shows successive structural phase transitions at $T_1=553$ K and at $T_c=403$ K which are analogous to those observed in Rb_2ZnCl_4 and Rb_2ZnBr_4 . The high-temperature phase ($T > T_1$) is paraelectric and the crystal structure is of the $\beta\text{-K}_2\text{SO}_4$ type which belongs to the orthorhombic space group $Pnma$ (D_{2h}^{16}) with $Z=4$ (Fig. 1). The intermediate phase ($T_1 > T > T_c$) is incommensurately modulated in the a direction like most of the members of this family. The low-temperature phase ($T_c > T$) is again commensurate and improper ferroelectric with a spontaneous polarization along the b axis. In this phase the unit-cell dimension is triplicated along the pseudo-hexagonal a axis with respect to the paraelectric high-temperature phase. The space group of this ferroelectric lock-in phase is $Pn2_1a$ (C_{2v}^9) with $Z=12$ as in the case of Rb_2ZnCl_4 and Rb_2ZnBr_4 .^{3,4} At T_c the incommensurate wave vector $\vec{q} = \frac{1}{3}(1-\delta)\vec{a}^*$ locks in at $\vec{q} = \frac{1}{3}\vec{a}^*$. In contrast to Rb_2ZnCl_4 and Rb_2ZnBr_4 , where δ is nearly constant below T_1 and decreases rapidly near T_c , in K_2ZnCl_4 δ decreases linearly with decreasing temperature.¹

K_2ZnCl_4 has been studied already by ^{35}Cl nuclear quadrupole resonance⁵ (NQR) and some information concerning the incommensurate phase was obtained. In the lock-in phase, however, too many lines were

missing to allow a correct interpretation of the NQR spectrum. In addition to this, new low-temperature phase transitions have recently been reported for some members of the $A_2\text{BX}_4$ family, such as Rb_2ZnCl_4 , Rb_2ZnBr_4 , and K_2ZnCl_4 .⁶⁻¹¹ These transitions lead from the lock-in phase to a new low-temperature phase with a still unknown structure. In order to gain more information about these two phases in K_2ZnCl_4 , we decided to repeat and complete the NQR measurements on a good single crystal.

^{35}Cl NQR MEASUREMENTS

All our NQR measurements were performed (i) on a DECCA superregenerative spectrometer and (ii) on a modified Bruker pulse spectrometer. In case (i) the sideband suppression method was used to avoid confusion with satellites coming from the quench frequency. The K_2ZnCl_4 single crystal was grown by slow evaporation of an aqueous solution of KCl and ZnCl_2 in a 2:1 molar mixture. The sample was heated or cooled by a nitrogen gas flow and the temperature accuracy was of the order of 0.5 K. No temperature hysteresis was observed in the spectra through the whole region of temperature. The ^{35}Cl NQR lines were followed from $T=580$ K down to $T=77$ K.

The temperature dependence of the ^{35}Cl NQR spectrum [Fig. 2(a)] shows evidence for three structural phase transitions: (a) at $T_1=553$ K,

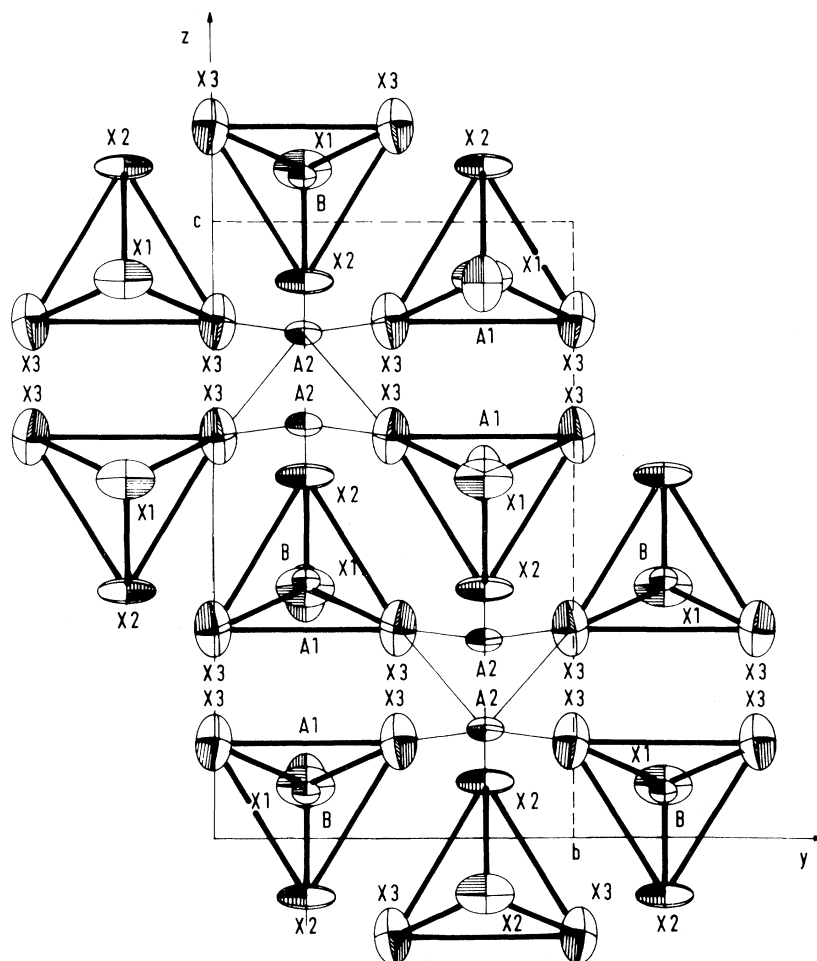


FIG. 1. Projection of the structure of the isomorphous Cs_2CdBr_4 crystal on the yz plane in phase I.

where the transition from the paraelectric phase to the incommensurate (IC) phase takes place, (b) at $T_{c_I} = 403$ K from the IC phase to the ferroelectric commensurate phase, and (c) at $T_{c_{II}} = 145$ K to the new low-temperature phase. This is illustrated in Table I where the four different phases are labeled as phase I, II, III, and IV.

In the paraelectric phase I [space group $Pnma$ (D_{2h}^{16}) with $Z=4$] there are only three chemically different Cl sites indicated by X_1 , X_2 , and X_3 in Fig. 1. Thus only three ^{35}Cl NQR lines (one per set) with an intensity ratio 1:1:2 are to be expected. However, only one of them could be detected. In the IC phase II this line splits into two edge singularities which can be followed only about 50 K down below T_I . About 20 K above T_{c_I} a new line appears which goes continuously into phase III.

In the lock-in phase III [space group $Pn2_1a$ (C_{2v}^9) with $Z=12$] there are 12 chemically inequivalent Cl sites. This is due to the triplication of the unit cell

and to the loss of the mirror plane m_y , which connected the two X_3 sites in phase I. Thus a total of 12 lines with equal intensities can be expected. Two groups of three lines, labeled X_1 and X_2 lines, could be detected with a good signal-to-noise ratio. However, from the six X_3 lines only one was observed. The procedure for assignment of the individual lines to the different sites X_i will be described in the discussion.

In the new phase IV a quadruplication of the X_1 lines could be observed [Fig. 2(b)]. Because of the rather broad lines in this phase, and numerous overlapping of the X_2 and X_3 lines, we were not able to resolve the spectrum properly for these sites. It is, however, not necessary to also prove the quadruplication for these lines, because in phase III all atoms are located on general positions and thus behave identically with respect to the line splitting.

Because of several effects, to be discussed, not all of the expected lines could be detected. To illustrate

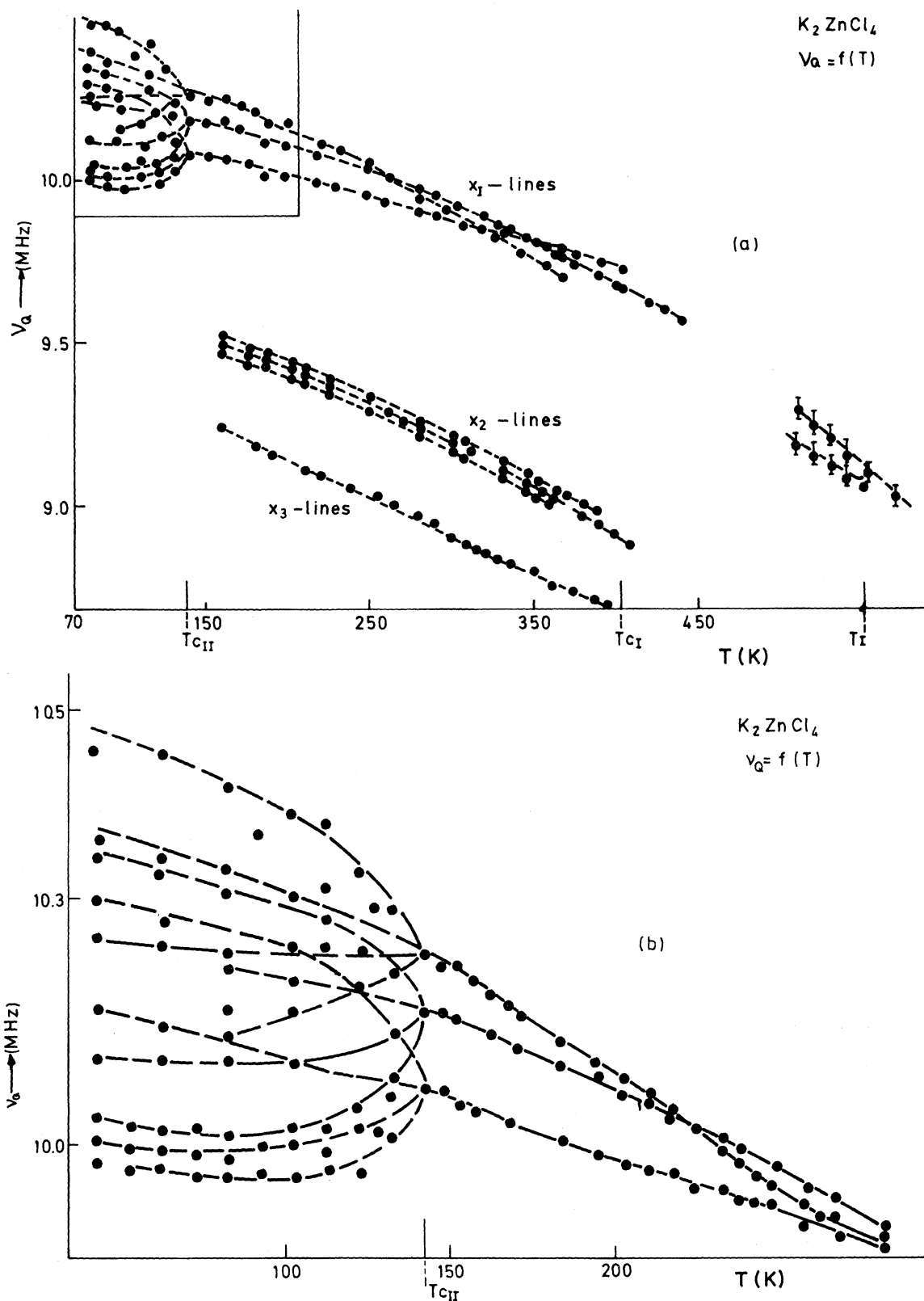


FIG. 2. Temperature dependence of the ^{35}Cl NQR frequencies in K_2ZnCl_4 : (a) all lines, (b) magnification of the upper left corner of (a).

TABLE I. Structural phase transitions.

Phase IV $T_{c_{II}} = 145$ K	Phase III $T_{c_I} = 403$ K	Phase II $T_I = 553$ K	Phase I
Polar (monoclinic) ($Z=24$)	Improper ferroelectric $Pn\ 2_1a$ (C_{2v}^2) $Z=12$	Incommensurate $\vec{q} = (1-\delta)\vec{a}^*/3$ $Z = \infty$	Paraelectric $Pnma$ (D_{2h}^{16}) $Z=4$

this feature, the signal-to-noise ratio of the strongest lines (the X_1 lines) is plotted as a function of temperature in the phases II, III, and IV (Fig. 3). One can also see that the X_1 lines become rather weak when approaching the transition temperatures T_{c_I} and $T_{c_{II}}$.

The soft-mode eigenvector of the transition I \rightarrow III (neglecting phase II) consists mainly of a rotation of the ZnCl_4 tetrahedra around the a axis and of displacements of the K atoms and the tetrahedra in the y direction. By means of Zeeman perturbed quadrupole resonance one can determine the rotation angles of the ZnCl_4 groups but not the displacements. In order to get a feeling for the magnitude of these rotations, a rotation pattern of the X_2 lines was performed in the lock-in phase III at $T=200$ K. This

temperature was chosen because only there the lines are narrow enough for this purpose. The magnetic field of 150 G was rotated in the yz plane of the crystal (Fig. 4).

DISCUSSION

Identification of the NQR lines in the lock-in phase III could be performed by taking into account the local symmetry of the ZnCl_4 groups, the pseudohexagonal structure of the crystal, as well as the symmetry properties of the nuclear quadrupole Hamiltonian.

Since the ZnCl_4 tetrahedra can be regarded as rigid and more or less regular, the principal axes z_i of the electrical field gradient (efg) tensors of the individual chlorine sites X_i have the direction of the

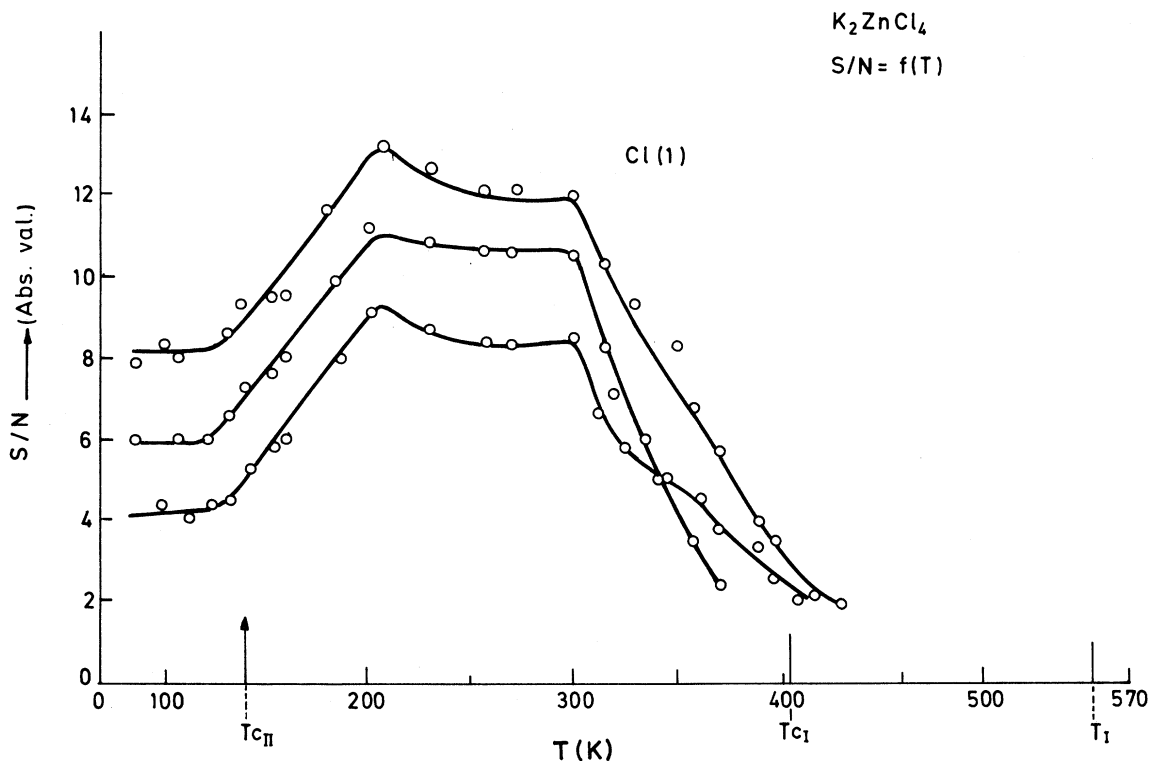


FIG. 3. Temperature dependence of the signal-to-noise ratio S/N for the ^{35}Cl NQR lines of the X_1 sites in K_2ZnCl_4 in the phases III and IV.

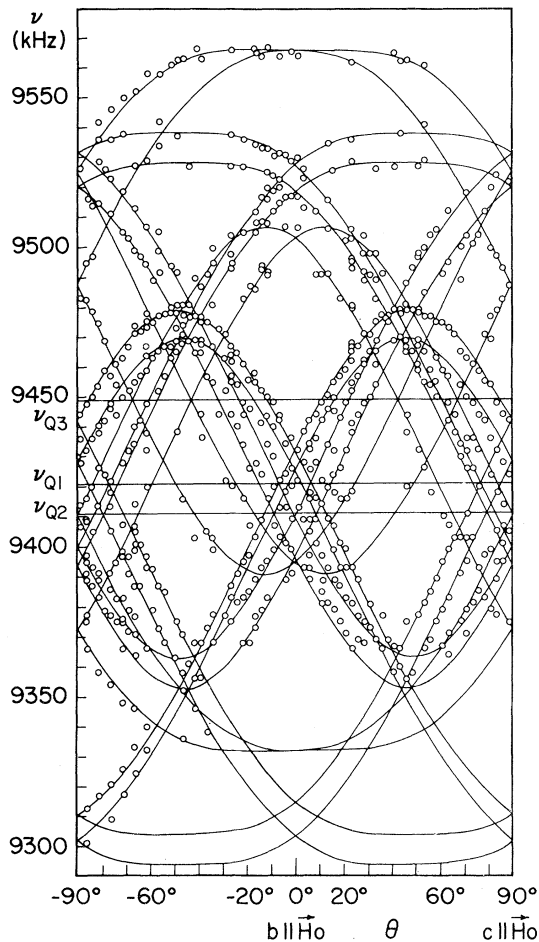


FIG. 4. Zeeman perturbed ^{35}Cl NQR rotation pattern of the three X_2 lines at 200 K. The magnetic field H_0 of 150 G was rotated in the yz plane of the crystal. The solid lines are calculated and the three horizontal solid lines indicate the unperturbed transition frequencies.

X_1 - B bonds, i.e., of the $\text{Cl}(i)$ - Zn bonds. Due to the pseudo-hexagonal symmetry of the orthorhombic phase I, all X_1 - B bonds are more or less parallel to the pseudo-hexagonal axis a . It is known that NQR transitions cannot be induced if the direction of the applied rf field is parallel to the quantization axis, which is parallel to the principal efg tensor axis z . Thus by putting the crystal into the rf coil with its a axis parallel to the coil axis, the X_1 lines should not be observed. By doing so, the three lines with the highest frequency were missing and could thus be assigned to the X_1 sites. For similar symmetry reasons,¹² the triplet in the middle can be assigned to the X_2 sites. From the six lines of the X_3 sites, only one could be observed.

In the paraelectric phase I, only the X_1 lines could be detected and followed into the IC phase II. Be-

cause the X_1 atom is located in the mirror plane, which is lost in phase II, the spontaneous part of the NQR frequency is a symmetric function of the order parameter η and thus of the displacements u_y .¹² In phase II the displacements are modulated along the a axis, so that no atom has the same displacement as another in the same column

$$u_y = \eta u_y^0 \cos[\phi(x)] .$$

Neglecting the higher-order terms of the symmetric function, the resonance frequencies of the individual sites depend in the following way upon the position x (Ref. 13):

$$\nu_Q = \nu_{Q_0} + \frac{1}{2} \nu_2 \cos^2[\phi(x)] ,$$

where ν_2 is proportional to η^2 . In the plane-wave limit, where $\phi(x)$ is proportional to x , one obtains the following distribution of resonance frequencies:¹²

$$f(\nu) \propto \left[\left| \frac{2(\nu - \nu_{Q_0})}{\nu_2} \right| \left| 1 - \frac{2(\nu - \nu_{Q_0})}{\nu_2} \right| \right]^{-1/2} .$$

This quasicontinuum spectrum has two edge singularities at

$$\nu_{(a)} = \nu_{Q_0}, \quad \nu_{(b)} = \nu_{Q_0} + \frac{1}{2} \nu_2 .$$

One thus expects a continuation of the "para" line into the IC phase, and an additional line which in the plane-wave limit should go continuously into the lock-in phase. This behavior was observed in the IC phase of Cs_2CdBr_4 and of Cs_2HgBr_4 .¹² If phase solitons are occurring, the intensity of the edge singularities is gradually transferred into commensurate lines already in the IC phase. In our case, however, the increasing amplitude of the modulation results in a widening of the spectrum, so that the intensity of the lines decreases below detectability. About 20 K above T_{c_1} one out of the three possible commensurate X_1 lines could be observed. We believe that this proves the existence of phase solitons in K_2ZnCl_4 . This line goes continuously through the lock-in transition, whereas the other two X_1 lines could be detected only somewhat below this transition.

The transition at $T_{c_{II}} = 145$ K is, within the precision of our measurements, a second-order transition; i.e., it is certainly of a distortive nature so that the Landau criteria can be applied. The line splitting is similar to that found in Rb_2ZnCl_4 below $T_{c_{II}}$.¹⁴ From the quadruplication of the X_1 lines [Fig. 2(b)] it can be concluded that the phase transition leads to a subgroup of index 4. The transition is thus either of the k_4 , t_4 , or k_2t_2 type. The k_4 type is an "equiclass" transition with a quadruplica-

tion of the unit cell, whereas the t_4 type is an equitranslational transition leading from the orthorhombic crystal class $mm2$ to the triclinic class 1. The third case k_2t_2 is a transition from $mm2$ to the monoclinic classes m or 2 with a doubling of the unit cell.

In Ref. 15 it is shown that the phase IV in Rb_2ZnCl_4 could be the result of the condensation of a doubly degenerate soft mode with wave vectors $q = \frac{1}{2}(b^* + c^*)$ and $q = \frac{1}{2}(b^* - c^*)$. These two branches belong to the triply degenerate soft mode in the hexagonal prototypic phase $P6_3/mmc$ (D_{6h}^4). It is well known that the $\beta\text{-K}_2\text{SO}_4$ structure $Pnma$ (D_{2h}^{16}) is essentially a pseudo-hexagonal structure. Actually the orthorhombic phase $Pnma$ can be looked upon as resulting from a distortive transition taking place in the hexagonal phase due to condensation of one out of these three soft-mode branches. The two other branches harden at this transition but remain degenerate in the phases I, II, and III. It is supposed that they become soft again at $T_{c_{II}}$. Such a mechanism would be in agreement with the second-order character of the III–IV transition. As a result of these considerations, three possible space groups for the phase IV of Rb_2ZnCl_4 were presented: $Pc11$ (C_s^2) with $Z=24$; $A11a$ (C_s^4) with $Z=24$; and $P1$ (C_1^1) with $Z=24$.

Combining these results (which hold also for the case of K_2ZnCl_4) with our NQR results, one is left with only two possible space groups $Pc11$ (C_s^2) and $A11a$ (C_s^4) both with $Z=24$. In Rb_2ZnCl_4 an additional spontaneous polarization was found in the direction of the pseudo-hexagonal a axis.¹⁶ This is only in agreement with the space group $A11a$ (C_s^4). In K_2ZnCl_4 , however, no additional polarization could be detected,¹⁷ so that both space groups are still possible for phase IV.

From the rotation pattern Fig. 4 the following results are obtained:

(i) The efg tensor of the X_2 site is axially symmetric within the precision of the measurements, displaying the still good regularity of the tetrahedra.

(ii) In deviation from Fig. 1, which shows the paraelectric phase of Cs_2CdCl_4 , the tetrahedra are tilted so that the bond X_2-B lies almost in the yz plane; i.e., the corresponding tilt angle is about 21° .

(iii) In the paraelectric phase the X_2-B directions lie in the mirror plane m_y . The maximum Zeeman splitting of the X_2 lines is thus reached for a magnetic field H_0 parallel to the c axis. From the angular shifts of the maxima away from this direction the rotation angles of the tetrahedra around the x axis can be obtained directly. These rotation angles are surprisingly large, i.e., $r_x = \pm 77.5^\circ$ for the uppermost line, $r_x = \pm 40.0^\circ$ for the middle line, and

$r_x = \pm 42.5^\circ$ for the lowest line. From this result the amplitude and phase of the lock-in wave can be obtained for rotation of the tetrahedra around the pseudo-hexagonal a axis.

Keeping in mind that the lattice period is tripled in phase III in the a direction with respect to phase I, one can see that any column of three atoms with the fractional coordinates (x, y, z) , $(x+1, y, z)$, and $(x+2, y, z)$ in phase I forms a set of chemically inequivalent atoms with different displacements u_x , u_y , and u_z in phase III. In the unit cell always four of these sets are related by the symmetry elements of the space group $Pn2_1a$. This is valid also for atom groups, so that we have four sets of ZnCl_4 tetrahedra in the unit cell which are related by symmetry elements. Within the set the tetrahedra are more or less aligned along the a direction but have different rotation angles. Knowing the x coordinate of the Zn atom of a selected tetrahedron in phase I, as well as the three rotation angles r_x within the set, one can calculate amplitude and phase of the frozen-in modulation for this set. From our data we obtain an amplitude $r_x^0 = 79^\circ$ and a phase $\phi = 3.3^\circ \pm 1.0^\circ$. The rotation r_x can be expressed by

$$r_x(x) = \bar{r}_x + r_x^0 \sin(2\pi x + \phi),$$

where $\bar{r}_x = 1.7^\circ$ is the average of the three rotation angles in the set.

Very recently the complete structure of the lock-in phase of Rb_2ZnCl_4 was determined by means of neutron diffraction.¹⁸ From these data one obtains much smaller rotations of the tetrahedra: $r_x^0 = 13.2^\circ$, $\phi = 13^\circ$. Also the tilting of the tetrahedra is about three times smaller with respect to K_2ZnCl_4 . This huge difference in the amplitude of the tetrahedron rotation may be the reason for the completely different behavior of the birefringence of the two compounds in phase III, although both have the same space group $Pn2_1a$ with $Z = 12$.¹⁹

It should be noted that a set contains an infinite number of atoms in the IC phase II. In this phase the sets are only connected by the fact that the corresponding modulation waves have the same amplitude and wave vector and that their phases are related. On approaching T_{c_1} a regular lattice of phase solitons is building up. These phase solitons are separating nearly commensurate translational 60° domains of the lock-in phase. This is demonstrated by the occurrence of commensurate lines in the NQR spectrum which do not change the frequency at the lock-in transition.

We shall now discuss the reasons for having regions where not all the lines could be detected. In the paraelectric phase I we are in a temperature region where it is already difficult to detect NQR sig-

nals at all because of the Boltzmann distribution of the spin states. In addition, there are slow fluctuations of the order parameter near T_1 . Since the eigenvector of the order parameter consists mainly of rotations of the ZnCl_4 tetrahedra around the a axis, the X_2 and X_3 sites are mainly affected, whereas for the X_1 sites the rotation occurs around the z axis of the efg tensor. For these sites the magnitude of the efg tensor fluctuations is small compared with those of the X_2 and X_3 sites. As a consequence, the X_1 line can still be observed when the X_2 and X_3 lines are already broadened. The same arguments also hold for the IC phase II.

In phase III a considerable line broadening is observed upon approaching either T_{c_1} or $T_{c_{II}}$. This line broadening reduces the signal-to-noise ratio S/N as shown in Fig. 3 for the X_1 lines. Again the effect shows up much more in the X_2 and X_3 lines. Since the line broadening is definitely not a T_1 effect (spin-lattice relaxation) in our case, it must either be a T_2 effect (spin-spin relaxation) or a static distribution of the resonance frequencies. A T_2 effect must have its origin in very slow motions because the spectral density $J(\omega=0)$ gives the relevant contribution to this relaxation. We assume that this is the case near $T_{c_{II}}$. Near T_{c_1} the line broadening could also be a consequence of a special domain pattern. If we assume that a substantial fraction of solitons survive the lock-in transition and remain as

domain walls, and that their number decreases with decreasing temperature, the linewidths would similarly decrease. This would explain the temperature dependence of the signal-to-noise ratio. Evidence for such domains has been observed in Rb_2ZnCl_4 by measuring the optical activity in both the IC phase II and the lock-in phase III.¹⁹ For symmetry reasons there should be no optical activity in the lock-in phase. The observed optical activity can only be explained by a domain pattern with domain sizes much smaller than the optical wavelengths. There is some evidence for a very slow relaxation of the domain pattern towards the equilibrium amount of domain walls.¹⁷ This mechanism could provide a considerable contribution to the spectral density $J(\omega=0)$ and hence affect the linewidth.

In conclusion, we can say that the combination of our NQR measurements with symmetry considerations and other information about the A_2BX_4 family yields a consistent picture of the microscopic properties of K_2ZnCl_4 and of the mechanism of its phase transitions. There are, however, still many open questions especially concerning the nature of the nonequilibrium states in phase III.

ACKNOWLEDGMENT

This work was supported in part by the Swiss National Science Foundation.

*On leave from J. Stefan Institute, E. Kardelj University of Ljubljana, 61001 Ljubljana, Yugoslavia.

¹K. Gesi and M. Iizumi, *J. Phys. Soc. Jpn.* **46**, 697 (1979).

²K. Gesi, *J. Phys. Soc. Jpn.* **45**, 1431 (1978).

³I. Mikhail and K. Peters, *Acta Crystallogr. B* **35**, 1200 (1979).

⁴K. Itoh, T. Kataoka, H. Matsunaga, and E. Nakamura, *J. Phys. Soc. Jpn.* **48**, 1039 (1980).

⁵F. Milia, *Ferroelectrics* **24**, 151 (1980); F. Milia and M. Voudouris, *Phys. Lett.* **76A**, 350 (1980).

⁶D. Kucharczyk, J. Kalicinska-Karut, and K. Lukaszewicz, Proceedings of the 6th European Crystallographic Meeting, Barcelona, Spain, 1980 (unpublished).

⁷I. A. Belobrova, I. P. Aleksandrova, and A. K. Moskalev, *Phys. Status Solidi A* **66**, K17 (1981).

⁸F. Milia, *Bull. Magn. Reson.* **1-4**, 247 (1980).

⁹M. Quilichini, J. P. Mathieu, M. Le Postollec, and N. Toupry, *J. Phys. (Paris)* **43**, 787 (1982).

¹⁰E. Francke, M. Le Postollec, J. P. Mathieu, and H. Poullet, *Solid State Commun.* **35**, 183 (1980); **33**, 155 (1980).

¹¹Th. Rasing, J. H. Stoelinga, P. Wyder, A. Janner, and T. Janssen, *Ferroelectrics* **26**, 707 (1980).

¹²S. Plesko, R. Kind, and H. Arend, *Phys. Status Solidi A* **61**, 87 (1980).

¹³R. Blinc, *Phys. Rep.* **79**, 5 (1981), and references therein.

¹⁴R. Kind, P. Mural, and E. Voit (unpublished).

¹⁵V. Dvorak and R. Kind, *Phys. Status Solidi B* **107**, K109 (1981).

¹⁶H. G. Unruh and J. Strömich, *Solid State Commun.* **39**, 737 (1981).

¹⁷H. G. Unruh (private communication).

¹⁸M. Quilichini and J. Parnetier, *Acta Crystallogr.* (in press).

¹⁹P. Günter and R. Sanctuary (unpublished).